CHAPTER 3

Basic principles and physics[1]

by: Albert Prak, MESA Research Institute, University of Twente, Enschede, the Netherlands

3.1 Introduction

Many different structures are used as resonating elements in resonant sensors. Examples are beams, diaphragms or membranes, the 'butterfly' structure, the 'H' structure, etc. (see review-tables in chapter 8). In such a resonator, many *types of vibrations* are possible (e.g. transversal, longitudinal, torsional and lateral vibrations). Since the structures generally have an infinite number of degrees of freedom (they have a distributed mass and spring-working), an infinite number of resonances, called *modes of vibration*, are possible for every vibration-type.

Since a large percentage of all resonant sensors comprise transversally vibrating prismatic beams, we focus our attention on such structures (prismatic beams are beams the flexural stiffness of which does not depend on the length coordinate). A further restriction concerns the boundary conditions of such a beam. We concentrate on a clamped-clamped microbridge, thus boundary conditions are: $v(x)=0$, $v'(x)=0$, $v(l)=0$ and $v'(l)=0$, where v is the deflection of the beam; see fig. 3.1. The boundary conditions of a clamped-free beam, for example, would be: $v(x)=0$, $v'(x)=0$, $v''(l)=0$ and $v'''(l)=0$

It should be emphasized that the solving methods outlined in the next sections are applicable to other types of vibrations and other structures with only minor changes. The transversal vibrations are very illustrative for a more general case.

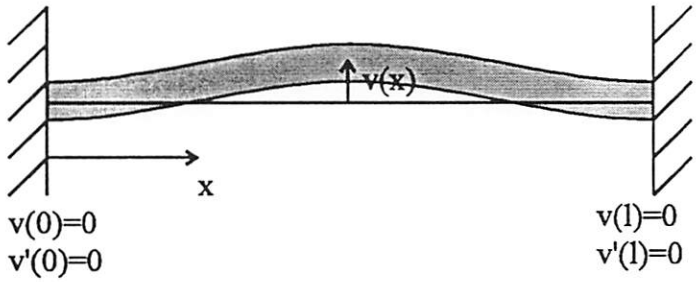

Fig. 3.1: Prismatic clamped-clamped microbridge

[1] Based on: A. Prak, *Silicon resonant sensors: Operation and response,* PhD-thesis, University of twente, Enschede, the Netherlands, 1993

3.2 The differential equation of a prismatic microbridge

Small transversal movements of a viscously damped prismatic microbridge subject to an axial force N and an externally applied driving load $P_e(x,t)$ (see fig. 3.2) are described by the following linear, inhomogeneous, partial differential equation, which is of the fourth order in space, and of the second order in time [3.1]:

$$\hat{E}_b I v''''(x,t) - N v''(x,t) + \varrho w_b h_b \ddot{v}(x,t) + c\dot{v}(x,t) = P_e(x,t) \qquad (3.1)$$

The symbols have the following meaning:

$v(x,t)$ the deflection to be solved
I the moment of inertia ($I=w_b h_b^3/12$)
c the viscous drag parameter (force per unit length per unit velocity)
w_b the width of the beam
h_b the thickness of the beam
$\hat{E}_b$ the apparent Young's modulus of the beam material, which equals $\hat{E}_b = E_b/(1-\nu_b^2)$ for beams with $w_b \gg h_b$. (ν_b is Poisson's ratio and E_b the Young's modulus)
ϱ the density of the beam material

Moreover, l is the length of the beam. A prime and a dot denote differentiation to x and t, respectively. In eq. (3.1) effects of rotary inertia and shear deformations, as well as nonlinear terms due to large amplitude vibrations have been neglected (Bernoulli assumptions).

In fact, eq. (3.1) describes the force equilibrium for every infinitesimal part dx of the beam. The various terms can be identified as follows. The first two terms describe the spring effect of the beam: its natural tendency to be uncurved. EI is called the flexural rigidity. Axially loaded beams ($N \neq 0$) show an additional term. The third term is correlated to the inertia of the beam: $\varrho w_b h_b$ is the mass per unit length, and $\ddot{v}(x,t)$ the acceleration. The fourth term is related to the velocity-proportional friction forces acting on the beam. Frictional forces which are proportional to other powers of the velocity are not considered here. Finally, the right hand side is related to the driving force acting on the beam: the force which sets the beam in motion. It is generated by one of the excitation mechanisms to be described in chapter 5.

We assume that separation of space and time coordinates is possible and that the time dependent parts of v and P_e are harmonic functions (an eventual static deflection and load is not considered in this chapter):

$$v(x,t) = \overline{v}(x)e^{j\omega t} \quad ; \quad P_e(x,t) = \overline{P}_e(x)e^{j\omega t} \qquad (3.2.a;b)$$

The overstrike is meant to indicate the (complex) amplitude of an harmonic quantity. Both the modulus and the phase of these quantities can depend on x. By factoring out the time

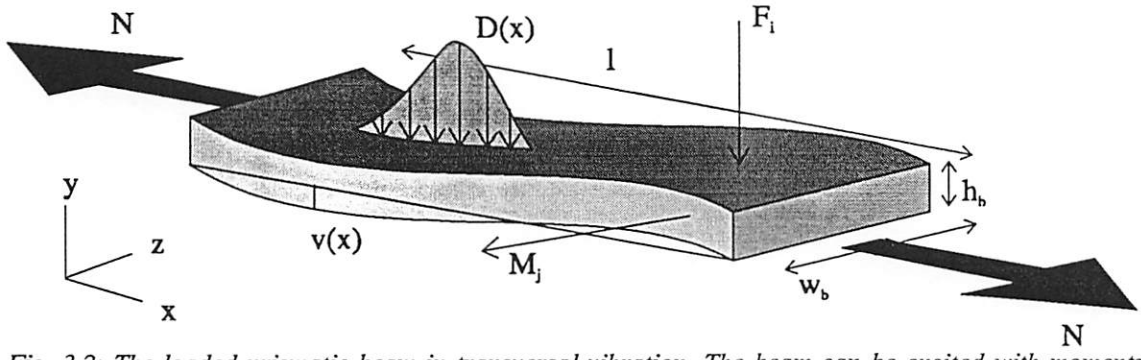

Fig. 3.2: The loaded prismatic beam in transversal vibration. The beam can be excited with moments and forces, which both can be concentrated or distributed.

dependent part, eq. (3.1) can be written as:

$$\hat{E}_b I \bar{v}''''(x) - N\bar{v}''(x) - (\omega^2 \rho w_b h_b - j\omega c)\bar{v}(x) = \bar{P}_e(x) \tag{3.3}$$

The beam can be excited with moments and forces, which both can be concentrated or distributed:

$$\bar{P}_e(x) = \bar{D}(x) + \sum_i \bar{F}_i \delta(x - x_i) - \bar{m}'(x) - \sum_j \bar{M}_j \delta_{-1}(x - x_j) \tag{3.4}$$

with

$\bar{D}$	a distributed force	(unit [N/m])
$\bar{F}$	a concentrated force	(unit [N])
$\bar{m}$	a distributed moment	(unit [Nm/m]=[N])
$\bar{M}$	a concentrated moment.	(unit [Nm])

Further, δ represents the Dirac delta function, and δ_{-1} its 'derivative', the unit doublet. $\bar{D}$ and $\bar{F}$ are directed exactly in the y-direction, and $\bar{m}$ and $\bar{M}$ are in the z-direction. By this assumption, the longitudinal, lateral and torsional vibrations are effectively ruled out. Only transversal vibrations will be excited.

3.3 Solving the homogeneous, undamped problem using Laplace transforms

The problem as stated in eqs. (3.3) and (3.4) is quite complicated. Nevertheless, it can be solved analytically if the right hand side is not to complicated. However, the resulting expressions for $v(x)$ are hopelessly complex mathematical functions, and give not much insight in the physics of the beam. Therefore, we will first solve the much simpler case of a undamped ($c = 0$) and undriven ($P = 0$) microbridge. The differential equation now becomes:

$$\hat{E}_b I v''''(x) - N v''(x) - \omega^2 \rho w_b h_b v(x) = 0$$

It can be solved analytically, for example by the following procedure:
- Laplace transformation of the differential equation.
- apply boundary conditions at x=0, which read $x(0)$=0 and $x'(0)$=0
- inverse Laplace transform yields the solution with 2 integration constants
- substitution of the boundary conditions at x=l ($x(l)$=0 and $x'(l)$=0) gives additional relations to eliminate these integration constants.

The differential equation can be rewritten conveniently by introducing the following parameters:

$$k^4 = \omega^2 \rho w_b h_b / \hat{E}_b I \tag{3.5}$$

$$p = N / 2\hat{E}_b I k^2 \tag{3.6}$$

$$k_1^2 = k^2\left(\sqrt{p^2 + 1} - p\right) \tag{3.7}$$

$$k_2^2 = k^2\left(\sqrt{p^2+1}+p\right) \tag{3.8}$$

$$H_1 = \cosh(k_2 l) - \cos(k_1 l) \tag{3.9}$$

$$H_2 = \sinh(k_2 l)/k_2 l - \sin(k_1 l)/k_1 l \tag{3.10}$$

$$H_3 = k_2 l \sinh(k_2 l) + k_1 l \sin(k_1 l) \tag{3.11}$$

$$H_4 = \cosh(k_2 l) - \cos(k_1 l) \tag{3.12}$$

Having introduced the above symbols, the homogeneous differential equation can be rewritten as:

$$v''''(x) - 2pk^2 v''(x) - k^4 v(x) = 0 \tag{3.13}$$

After transformation to the s (Laplace) domain we obtain:

$$s^4 V(s) - s^3 v(0) - s^2 v'(0) - s v''(0) - v'''(0) - 2pk^2 s^2 V(s) + 2pk^2 s v(0) + 2pk^2 v'(0) - k^4 V(s) = 0$$

where $V(s) = \mathcal{L}\,\bar{v}(x)$ is the Laplace transform of $\bar{v}(x)$. Applying boundary conditions at $x = 0$ ($v(x) = 0$, $v'(x) = 0$) gives:

$$s^4 V(s) - s v''(0) - v'''(0) - 2pk^2 s^2 V(s) - k^4 V(s) = 0$$

or

$$V(s)\left(s^4 - 2pk^2 s^2 - k^4\right) = sC_2 + C_3$$

where $C_2 = v''(0)$ and $C_3 = v'''(0)$. We can rewrite:

$$V(s) = \frac{1}{l^2}\frac{1}{k_1^2 + k_2^2}\left(\frac{1}{s^2 - l^2 k_2^2} - \frac{1}{s^2 + l^2 k_1^2}\right)\left(s v''(0) + v'''(0)\right)$$

with k_1 and k_2 as defined in eqs. (3.7) and (3.8). This explicit relation in $V(s)$ can be inverse transformed (using a table with Laplace transforms) to give:

$$v(x) = \frac{1}{l^2(k_1^2 + k_2^2)}\left[C_2\left(\cosh(k_2 x) - \cos(k_1 x)\right) + C_3\left(k_2 \sin(k_1 x) - k_1 \sinh(k_2 x)\right)\right] \tag{3.14}$$

To eliminate either C_2 or C_3, we have to apply the boundary conditions at $x = l$. (so this is the point were the route of clamped-clamped and clamped-free beams splits up). We find:

$$\begin{cases} C_2 H_1 + C_3 H_2 = 0 \\ C_2 H_3 + C_3 H_4 = 0 \end{cases}$$

where H_1 through H_4 are defined by eqs. (3.9)-(3.12). The upper equation is found by substitution of $v(l) = 0$ in eq. (3.14), while the lower equation is found by differentiating eq. (3.14) with respect to x, and apply the other boundary condition ($v'(l) = 0$). The above set obviously has solutions only if:

$$H_2 H_3 - H_1 H_4 = 0$$

After some calculations it is found that solutions only exist if:

$$\cos(k_1)\cosh(k_2)+\frac{1}{2}\left(\frac{k_1}{k_2}-\frac{k_2}{k_1}\right)\sin(k_1)\sinh(k_2)-1=0 \tag{3.15}$$

This is the so called *frequency condition*. Solving this implicit relation in the angular frequency ω (both k_1 and k_2 are functions of ω) leads us to a discrete number of real frequencies: the eigenfrequencies or resonance frequencies. Solutions can generally be written as:

$$\omega_i = 2\pi n_i \sqrt{\frac{\hat{E}}{\varrho}\frac{h}{l^2}}$$

If there is no axial force ($N = 0$), both k_1 and k_2 equal k. In that case, the first five resonance frequencies are given in table 3.1. These values, as well as the values for structures with different boundary conditions can also be found in [3.2]

Table 3.1: First five resonance frequencies of an axially unloaded microbridge

	$i=1$	$i=2$	$i=3$	$i=4$	$i=5$
n_i	1.028	2.834	5.555	9.182	13.72

The dependence of the resonance frequencies on the axial load, which is of importance if the resonator is used as an resonant strain gauge, will be treated in one of the next sections: Response of silicon resonant sensors.

In deriving the frequency condition, another relation, is found by which either C_2 or C_3 can be eliminated from eq. (3.14):

$$C_3 = -C_2\frac{\cosh(k_2 l)-\cos(k_1 l)}{\frac{1}{k_2 l}\sinh(k_2 l)-\frac{1}{k_1 l}\sin(k_1 l)}$$

so the final solution for the shape of the beam at resonance reads:

$$v(x)=\frac{C_2}{l^2(k_1^2+k_2^2)}\left[\cosh(k_2 x)-\cos(k_1 x)+\frac{\cosh(k_2 l)-\cos(k_1 l)}{k_1\sinh(k_2 l)-k_2\sin(k_1 l)}\left(k_2\sin(k_1 x)-k_1\sinh(k_2 x)\right)\right] \tag{3.16}$$

Eq. (3.16) describes the shape of the beam in resonance. The functions $v(x)$ are often called the *mode shape* functions. For the clamped-clamped beam, the mode shapes are quite complex: the shape consists of a linear combination of the functions sin, cos, sinh and cosh. The first five mode shape functions are shown in fig. 3.3.

The beam can be compared very well to a stretched wire (a guitar string). In this much simpler case, the resonance frequencies are given by the simple equation $\omega_i = i\,\omega_1$ (where ω_1 is

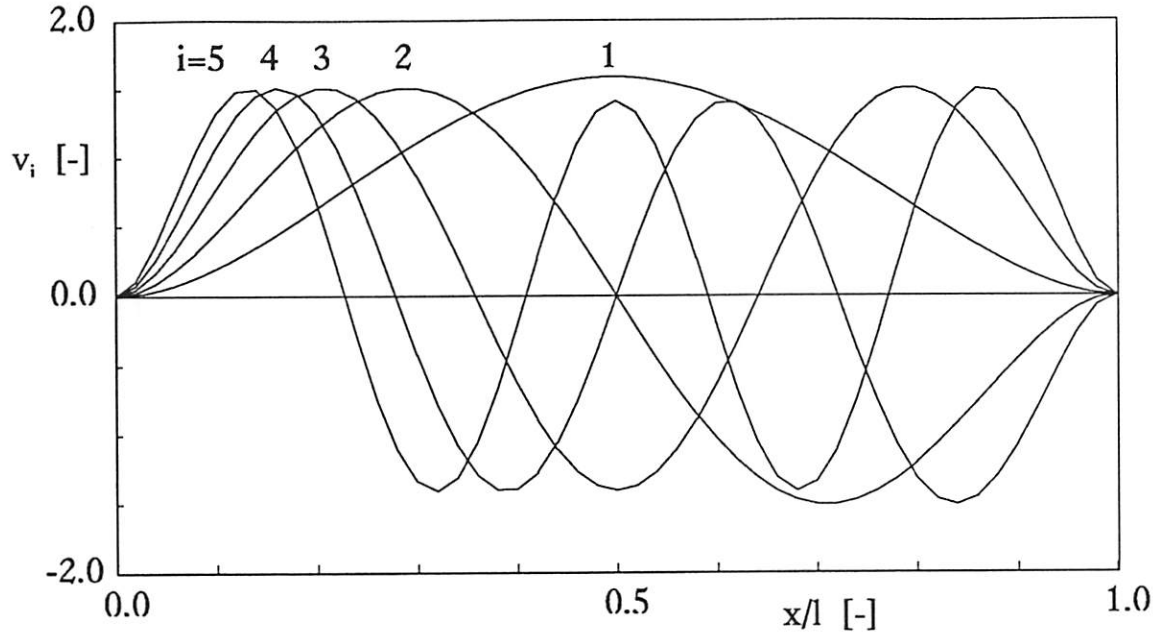

Fig. 3.3: First 5 normalized mode shapes of an unstrained microbridge computed at 50 equidistant points. Note that the values of the extrema of the modes are nearly equal. For mode 1 to 5 they are 1.588, 1.510, 1.512, 1.512 and 1.512 respectively.

the lowest resonance frequency and i the mode number) and the mode shapes by $v(x) = C \sin(i\pi x/l)$

Now, we have solved the homogeneous problem. As mentioned earlier, the inhomogeneous problem (that is a microbridge driven by a harmonic force / moment, i.e. the right hand side of eq. (3.1) ≠0) can also be solved using the procedure outlined above, provided that the drive functions are not too complicated. However, the results are hopelessly complex mathematical expressions and do not give much insight in the physics of the beam. Therefore, a much more elegant method is used to describe the driven microbridge.

3.4 Solving the inhomogeneous problem by modal analysis

$$\psi = \sum_{i=1}^{\infty} C_i \cdot \phi_i$$

If the beam is driven (by some wild excitation function) and its vibration is damped, it can show any arbitrary (continuous) shape obeying the boundary conditions (see e.g. fig. 3.4). The set of modeshape functions prove to be an independent (orthogonal) set of functions: every arbitrary shaped beam can be written as a sum of the modeshape functions. This is a central statement in a technique called modal analysis [3.3]. Meirovitch 1967

Thus the solution of the general differential equation, eq. (3.3), can be written as the

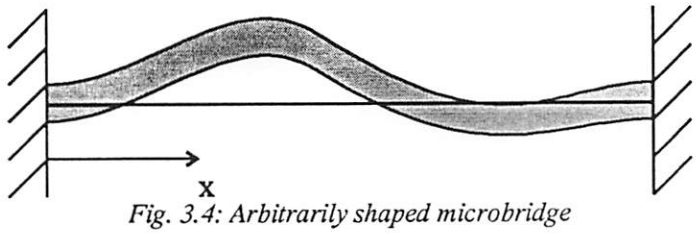

Fig. 3.4: Arbitrarily shaped microbridge

following expansion series:

$$\bar{v}(x) = \sum_{i=1}^{\infty} \bar{y}_i v_i(x) \qquad (3.17.a)$$

In this equation, $v_i(x)$ are the *mode shapes*, and y_i are the *modal coordinates*. (also called *generalized coordinates*). They tell us how strong mode i is represented in the vibration. The shape of the beam of fig. 3.4, for example, can be obtained by using the first two mode shapes. The shape is clearly a-symmetrical, which is a result of a rather strong contribution of the second mode. On the average, the beam is lifted above the $y = 0$ plane. This is a result of the first mode shape. Hence, y_1 and y_2 are rather large. Higher modes do not contribute significantly: y_3 through y_∞ are small.

The modal analysis strongly reminds us of the Fourier analysis. However, in modal analysis the mode shapes are used as a set of base functions, rather than the sin and cos functions in the case of a Fourier analysis. Just like in a Fourier series, eq. (3.17) has its inverse equation:

$$\bar{y}_i = \frac{1}{l}\int_0^l \bar{v}(x) v_i(x) dx \qquad (3.17.b)$$

Very important properties of the mode shapes are that they are *orthogonal* and that they form a *complete* set (otherwise the Fourier-like expansion were not possible), that is: *any* function satisfying the boundary conditions can be expanded in the mode shapes. This means that vibrations at whichever axial load and damped by whichever (non-viscous) mechanisms can be expanded in the mode-shape functions (put up for a specific axial load) in one unambiguous way. The orthogonality of the modes is expressed in eq. (3.18), which also defines the aforementioned normalization of the modes.

$$\frac{1}{l}\int_0^l v_i(x) v_j(x) dx = \delta_{i,j} \qquad (3.18)$$

where δ_{ij} is the Kronecker delta.

After some mathematical operations, the original differential equation, eq. (3.1), can be rewritten in a modal representation (see e.g. [3.3]):

$$M_i \ddot{\bar{y}}_i + R_i \dot{\bar{y}}_i + K_i \bar{y}_i = \bar{P}_{e,i} \qquad i=1,2,... \qquad (3.19)$$

M_i, R_i and K_i denote the *modal mass*, *modal damping-constant* and *modal spring-constant* respectively, for which the following expressions hold:

$$M_i = \varrho w_b h_b l \quad ; \quad R_i = cl \quad ; \quad K_i = \varrho w_b h_b l \omega_i^2 \qquad (3.20.a;b;c)$$

$\bar{P}_{e,i}$ are the *modal (generalized) loads*. $\bar{P}_{e,i}$ are a measure for the efficiency with which a specific mode is excited. They are the expansion coefficients of the total load:

$$\bar{P}_{e,i} = \int_0^l \bar{P}(x) v_i(x) dx \quad ; \quad \bar{P}(x) = \frac{1}{l}\sum_{i=1}^{\infty} \bar{P}_{e,i} v_i(x) \qquad (3.21.a;b)$$

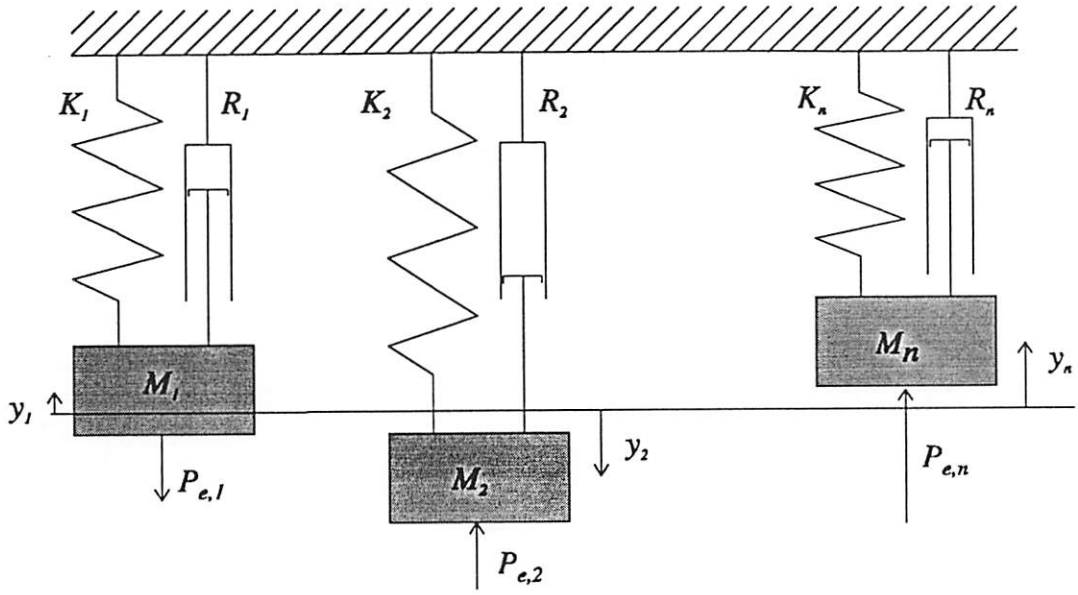

Fig. 3.5: Representation of the distributed beam by an infinite number of lumped elements.

From eq. (3.19) it is seen that the system can be described as an infinite number of independent systems, every one of which can be described by a standard equation of motion of second order in time. This is vizualized in fig. 3.5. The solution of a particular mode can easily be found from eq. (3.19) and equals:

$$\bar{y}_i = \frac{\bar{P}_{e,i}/K_i}{1 + j\frac{1}{Q_i}\frac{\omega}{\omega_i} - \left(\frac{\omega}{\omega_i}\right)^2} \tag{3.22}$$

where Q_i is the modal quality factor, defined by:

$$Q_i = \sqrt{M_i K_i}/R_i = \frac{M_i}{R_i}\omega_i \tag{3.23}$$

For a viscously damped beam, the ratio M_i/R_i does not depend on the mode number. It can be interpreted as the decay time of the vibration.

Summary:

In this section, it was shown that the distributed beam can be represented by an infinite number of independent simple second order systems with concentrated elements. Every element corresponds to a mode of vibration. A mode is completely characterized by a mass M_i, a friction coefficient R_i, a spring constant K_i, a modal coordinate y_i and a modal force $P_{e,i}$. These quantities are connected to the real physical system (the beam) by eqs. (3.20.a;b;c), (3.17.b) and (3.21.a) respectively. Q_i can also be used instead of R_i (eq. (3.23)).

3.5 Finite element method (FEM)

The modal analysis method gives a good physical insight in the vibrating elements. Moreover, the method is very simple to apply once the modes of vibration are known. Very accurate results can be obtained with only a few modes taken into account. Usually, resonant sensors are operated at (or near) resonance, so in many cases it is justified to model the resonator with one or a few modes.

However, to find the vibration modes, a rather complex procedure has to be followed (see section 3.3). For simple structures, like a clamped-clamped bridge, the modes can be found analytically. If the structure is not this simple (e.g. a membrane, a non-prismatic beam) it can be very difficult (or even impossible) to find the mode shapes and corresponding resonance frequencies. In that case, the use of finite element programs is recommended.

Lots of commercial finite element programs are available on the market. We will not go into detail about finite element programs here (examples will be given in chapter 7), but the key to the solution is that the resonator is geometrically divided into a number 'finite elements', (see fig. 3.6). After specifying material properties, boundary conditions and loads, these programs are able to solve the strains and displacements of the elements. Every element can be deformed in a particular way. Corresponding strains and stresses can then be calculated. Important condition is that the edges (nodes) of one element should always coincide with the nodes of the neighbouring element. Final results are found using matrix equations which minimize the total energy of the system.

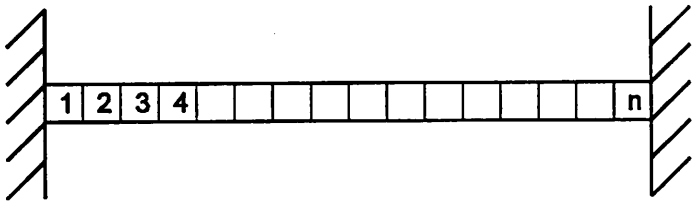

Fig. 3.6: Division of the structure in a number of finite elements.

3.6 Response to axial loads

In section 3.3, the resonance frequency of an axially unloaded microbridge is given. In a resonant strain gauge, the fact that the resonance frequency depends on the axial load is exploited, so we are interested in the relation between the axial load and the resonance frequency. The resonance frequency of an arbitrary mode, say the i-th mode, can be obtained from the implicit relation eq. (3.15). This equation can only be solved numerically. The solution is graphically represented in fig. 3.7. In this figure, the stress is normalized with respect to the buckling stress (the buckling stress is the compressive stress at which an ideal microbridge buckles; for the buckling stress holds: $\sigma_{buck} = -3.290\, \hat{E}_b h_b^2/l^2$) thus $\hat{\sigma} = -\sigma / \sigma_{buck}$. For stresses below $\hat{\sigma} = -1$ the bridge buckles, and the model is not valid anymore. The ratio of the resonance frequencies as a function of the normalized stress is given in fig. 3.8. This figure is very useful for characterization purposes (determination of intrinsic stress due to additional layers/materials), or for identification of modes.

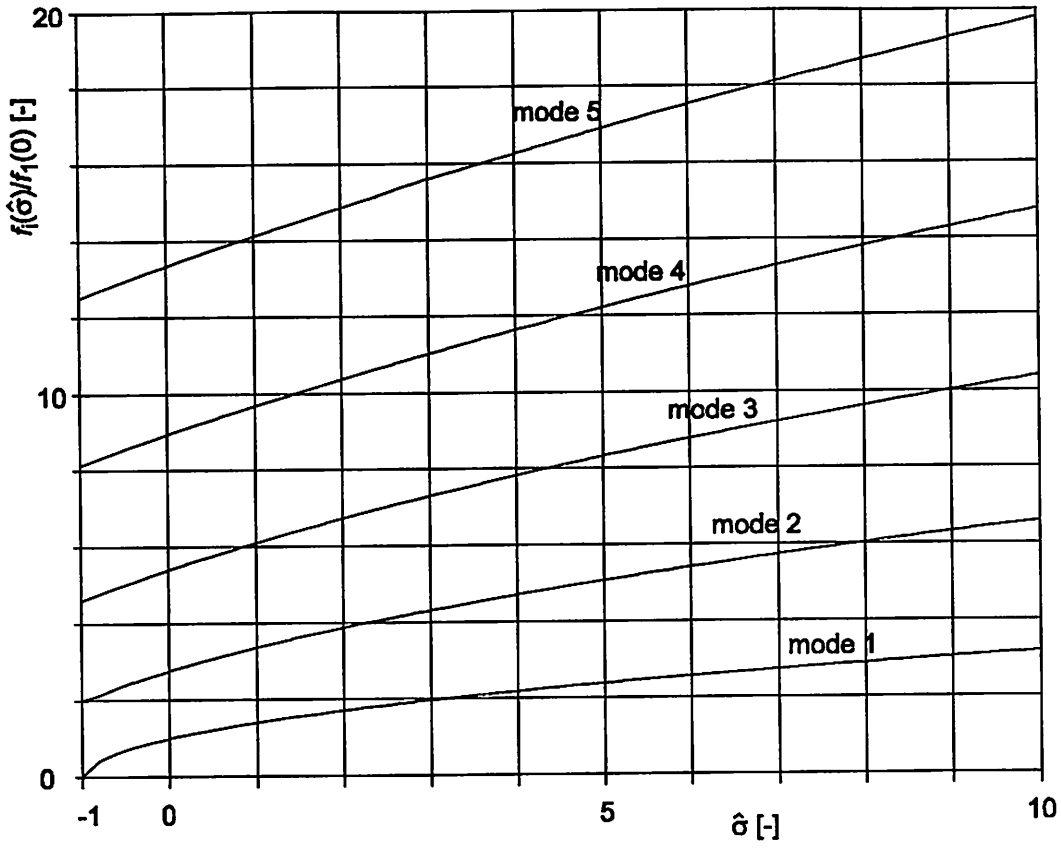

Fig. 3.7: Resonance frequency as a function of the normalized stress for the first five modes of a microbridge. The frequencies are normalized with respect to the stress free resonance frequency of the first mode.

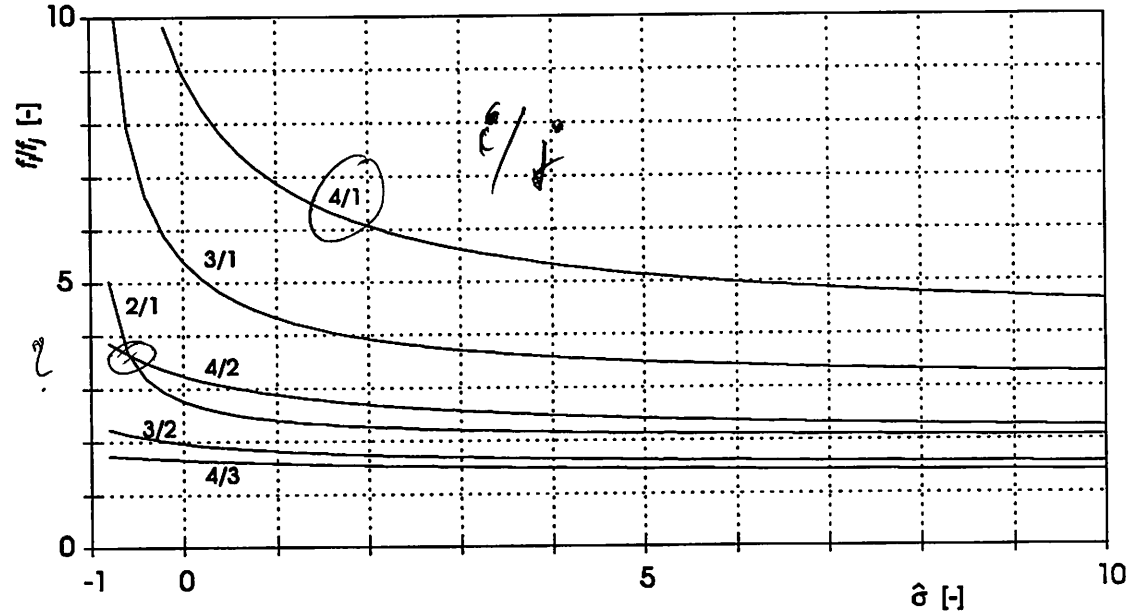

Fig. 3.8: Ratio of resonance frequencies as a function of the normalized stress

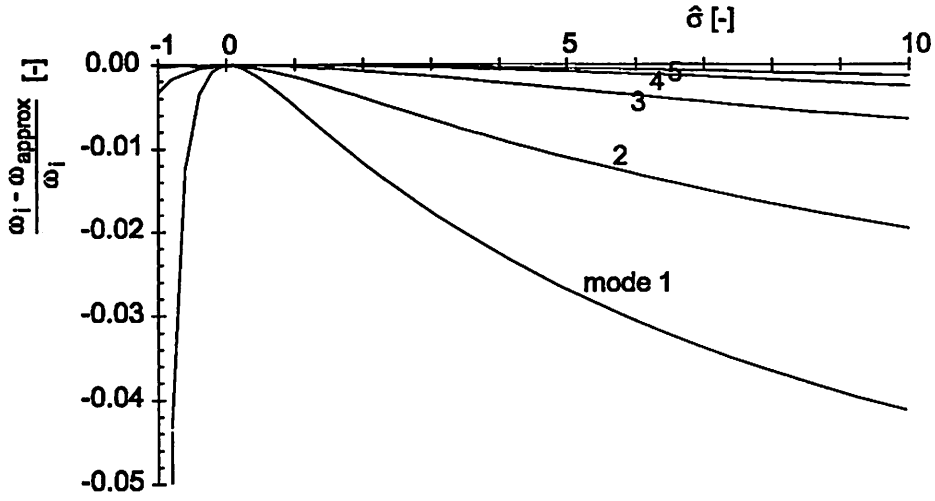

Fig. 3.9: Relative difference between numerically determined resonance frequency and the approximated resonance frequency for the first five modes of a microbridge according to table 3.2.

Note that for large σ, the asymptote of the curves is given by the ratio of the numbers of the modes involved. This is because the beam behaves as a stretched wire for large stresses.

The relation between the resonance frequency and the axial load is far from linear. However, in good approximation, this relation satisfies a square-root relation, thus the relation $f_i^2 \propto \sigma$, is almost linear. In a sensor environment, the non-linearity of this relation can be compensated for by a data processing unit. The axial load can then be calculated from the resonance frequency using an algorithm, or a look-up table. In the first case, an accurate knowledge of the non-linearity of the axial load-frequency relation is necessary.

The square-root relation is conveniently written as:

$$f_i = f_{0,i}\sqrt{1+\gamma_i\hat{\sigma}} \tag{3.24}$$

where $f_{0,i}$ is the resonance frequency without an axial load applied:

$$f_{0,i} = \alpha_i\sqrt{\frac{\hat{E}_b}{\varrho}}\frac{h_b}{l^2} \tag{3.25}$$

The coefficients α_i and γ_i obtained by fitting f_i and $df_i/d\sigma$ at $\sigma = 0$ are listed in table 3.2. The curve can also be fitted using other criteria, for example by fitting f_i at $\sigma = 0$ and at $\sigma = \sigma_{buck}$. In that case, different coefficients will be found for γ_i.

Table 3.2: Coefficients of approximated calibration curve (see eqs. (3.24) and (3.25))

mode	α_i	γ_i
1	1.028	0.9702
2	2.834	0.4780
3	5.555	0.2671
4	9.182	0.1696
5	13.72	0.1169

The relative difference between the approximated resonance frequency, using the coefficients of table 3.2, and the actual resonance frequency are given in fig. 3.9. For the first

mode, a difference of a few percent is found for stresses as low as a few times the buckling stress.

When the bridge has a small initial deflection, deviations from the behaviour as sketched in fig. 3.7 can occur in the negative stress region [3.4], see fig. 3.10.

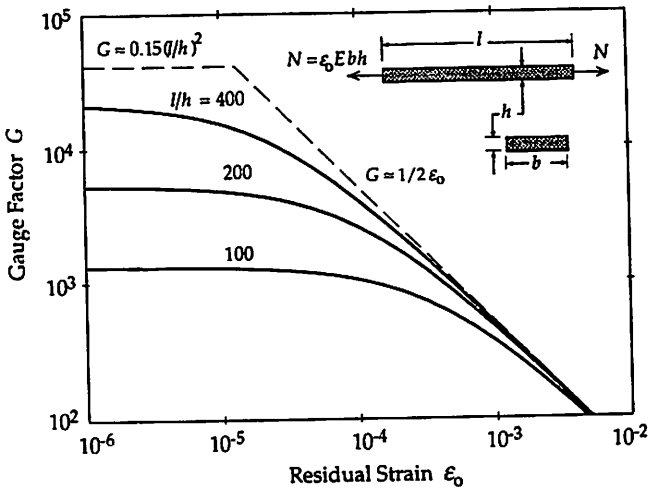

Fig. 3.10: Resonance frequency of a non-ideal microbridge. This behaviour deviates from the behaviour as sketched in fig. 3.7. Figure from [3.4]

3.7 Gauge factors

The normalized sensitivity of the sensor output signal with respect to the measurand is often referred to as the gauge factor. in the case of a conventional (piezoresistive) strain gauge, for examples, the gauge factor is defined as:

$$G = \left(\frac{1}{R_0} \frac{dR}{d\varepsilon} \right)_{\varepsilon_0}$$

where R_0 is the resistance at zero strain, and $dR/d\varepsilon$ is the change in the resistance per unit strain at a particular reference strain ε_0. For resonant strain gauges, a gauge factor can be defined in a similar way:

$$G = \left(\frac{1}{f_0} \frac{df}{d\varepsilon} \right)_{\varepsilon_0} \tag{3.26}$$

Using the expression for the resonance frequency, eq. 3.24, the gauge factor can be written as:

$$G = \frac{1}{2} \left(\frac{\gamma_i (l/h)^2}{1 + \gamma_i \varepsilon_0 (l/h)^2} \right)$$

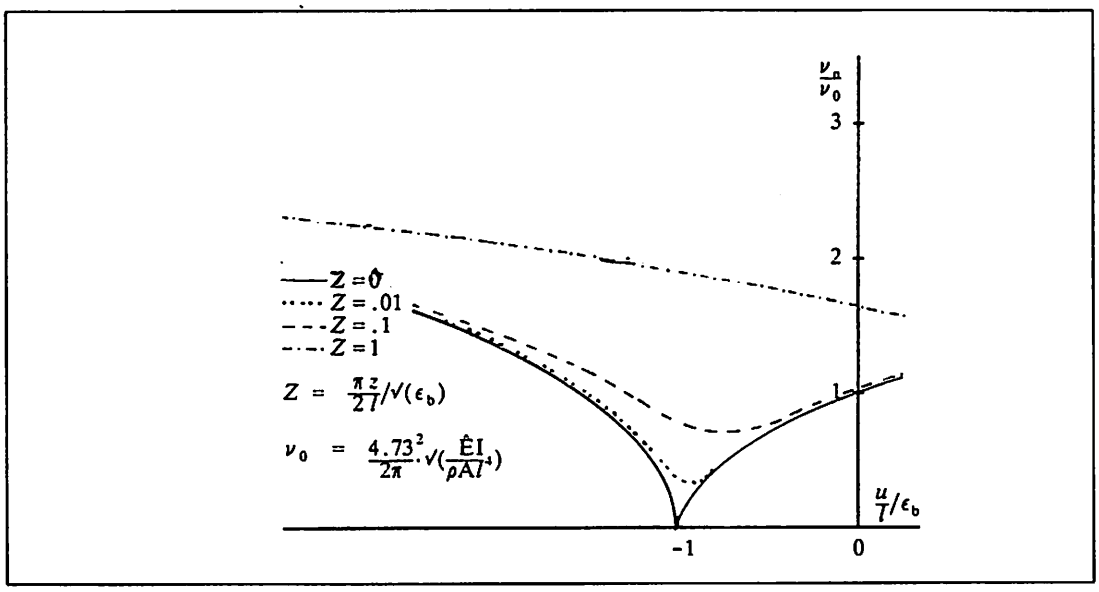

Fig. 3.11: Gauge factor for the first mode of a microbridge as a function of the strain for three values of the length to thickness ratio l/h. Fig. from [3.5]

For the first mode, the gauge factor is graphically represented in fig 3.11. The parameter *l/h* is very important with respect to gauge factors. With today's fabrication technologies, *l/h* ratio's of 100 are easily obtained, and ratio's of 1000 are possible. This results in very high stress sensitivities as compared to the gauge factors of e.g. piezoresistive strain gauges, which are typically 100 for silicon strain gauges, and much lower for metal ones.

For very high stresses (which can be the result of either the intrinsic stress due to the fabrication process or the measurand) the bridge behaves as a stretched wire. In this case the resonance frequency exactly obeys:

$$f_i = \frac{i}{2l}\sqrt{\frac{\sigma}{\rho}} \tag{3.27}$$

References

[3.1] S.P. Timoshenko, D.H. Young and W. Weaver, *Vibration problems in engineering*, John Wiley & Sons, 4th ed. (1974), Ch 5.

[3.2] R.D. Blevins, *Formulas for natural frequencies and mode shapes*, Van Nostrand Reinhold, New York, 1979.

[3.3] L. Meirovitch, *Analytical methods in vibrations*, Collier-Macmillan Ltd., London (1967).

[3.4] S. Bouwstra and B. Geijselaers, *On the resonance frequencies of microbridges*, IEEE Proc. 6th Int. Conf. Solid State Sensors and Actuators (Transducers 91), 24-27 June 1991, San Fransisco CA USA, 538-542.

[3.5] H.A.C. Tilmans, M. Elwenspoek and J.H.J. Fluitman, *Micro resonant force gauges*, Sensors and Actuators A, 30 (1-2) 1992), 35-53.